JOURNAL OF MATERIALS SCIENCE **37** (2002) 4537–4543

# Preparation of calcium aluminate matrix composites by combustion synthesis

H. C. YI, J. Y. GUIGNÉ
*Guigné International Ltd, Paradise, NF, Canada A1L 1C1, Canada*
*E-mail: hcyi@guigne.com*

J. J. MOORE, F. D. SCHOWENGERDT
*Center for Commercial Applications of Combustion in Space (CCACS), Colorado School of Mines, Golden, CO 80401, USA*

L. A. ROBINSON, A. R. MANERBINO
*Guigné International Ltd, Paradise, NF, Canada A1L 1C1, Canada*

$CaO–Al_2O_3–TiB_2$ composites have been produced by the Combustion Synthesis technique. These materials have matrices based on binary calcium-aluminate compounds, i.e., $Ca_3Al_2O_6$ ($C_3A$), $Ca_{12}Al_{14}O_{33}$ ($C_{12}A_7$), $CaAl_2O_4$ (CA), $CaAl_4O_7$ ($CA_2$) and $CaAl_{12}O_{19}$ ($CA_6$). Except for samples with the matrix composition of $C_3A$, the combustion synthesis reactions can be characterized as stable self-propagating waves with combustion temperatures ranging from 2125 K to 2717 K and combustion wave velocity from 4.0 mm/s to 10.6 mm/s. For samples with a matrix composition of $C_{12}A_7$, CA, and $CA_2$, predominantly equilibrium compound phase was formed, while for samples with a matrix composition of $C_3A$, non-equilibrium phases were also present. There was no evidence of $CA_6$ formation for samples with a matrix composition corresponding to $CA_6$.


## 1. Introduction

Calcium aluminates ($CaO–Al_2O_3$) are attractive ceramic materials for high temperature refractory applications. They also play important roles in the steel industry as metallurgical slags and in cement technology as hydraulic materials. In recent years, there has been renewed interest in their capability of glass formation both for practical and scientific reasons. Calcium aluminate glasses have infrared (IR) transmissions up to 6 $\mu$m, which is superior to ordinary oxide glasses [1]. They are scientifically important too since they do not contain any of the usual glass-forming ions, and therefore the traditional network glass-forming theories are not applicable.

The phase diagram of the system is shown in Fig. 1 [2, 3]. There are five calcium aluminate compounds in the system, namely, $Ca_3Al_2O_6$($C_3A$), $Ca_{12}Al_{14}O_{33}$ ($C_{12}A_7$), $CaAl_2O_4$ (CA), $CaAl_2O_7$ ($CA_2$), and $CaAl_{12}O_{19}$ ($CA_6$). Properties of these compounds are listed in Table I. Calcia (CaO) has a melting point of 3173 K. When alumina is first added in, the $C_3A$ compound is precipitated out while the melting temperature of the mixture drops continuously in the process. The pure $C_3A$ compound melts incongruently at 1817 K. Further increase of alumina leads to the further decrease of melting points and formation of a new compound, $C_{12}A_7$, which has a melting temperature of 1722 K. Initially, it was suggested that this compound was unstable in the anhydrous $CaO–Al_2O_3$ system [4, 5]. However, there seems to be no doubt of its existence and it was synthesized in many studies in recent years [3, 6–8]. If more alumina is added to the mixture continuously, the melting points start to rise and the compounds of CA, $CA_2$ and $CA_6$ form respectively. The CA, $CA_2$ compounds melt congruently at 1873 K and 2048 K, respectively, while the $CA_6$ compound melts incongruently at 2156 K. The pure alumina ($\alpha$-$Al_2O_3$) melts at 2327 K. The thermodynamic properties of these compounds were evaluated by Hallstedt [3], and by Eriksson and Pelton [9]. The standard heat of formation ($\Delta H_f^{298}$) data for these compounds shown in Table I, relative to the pure CaO and $Al_2O_3$ oxides, are from Hallstedt [3].

The crystal structures of these compounds are also listed in Table I. They are used as references to index the X-ray diffraction spectra in the present work.

The traditional technique of preparing the calcium aluminate compounds is by solid state reactions (sintering) between calcia (CaO), or calcium carbonate ($CaCO_3$) and alumina ($Al_2O_3$) powders at temperatures in excess of 1673 K for a long period of time in order to obtain the single phase desired. Singh *et al*. [6] used this technique to study the reaction kinetics of $C_3A$, CA, and $CA_2$ compounds. It was found that when the powder mixture was heated to the temperature range 1473–1673 K, all of the thermodynamically stable compounds were initially formed. The single equilibrium phase could be obtained only after a prolonged reaction

TABLE I Properties of calcium-aluminate compounds

| Compounds | $T_m$ (K) | Crystallography | $\Delta H_f^{298}$ (kJ mol$^{-1}$)[a] |
|---|---|---|---|
| $Ca_3Al_2O_6$ ($C_3A$) | 1817 | Cubic, Space group Pa3 [10] | −5.2 |
| $Ca_{12}Al_{14}O_{33}$ ($C_{12}$ $A_7$) | 1718 | Cubic, Space group I-43d [11] | −76.2 |
| $CaAl_2O_4$ (CA) | 1873 | Monoclinic, Space group $P2_1/n$ [12] | −15.5 |
| $CaAl_2O_7$ ($CA_2$) | 2048 | Monoclinic, Space group C2/c [12] | −11.8 |
| $CaAl_{12}O_{19}$ ($CA_6$) | 2156 | Hexagonal, Space group P63/mmc [13] | −22.2 |

[a]From Hallstedt [3].

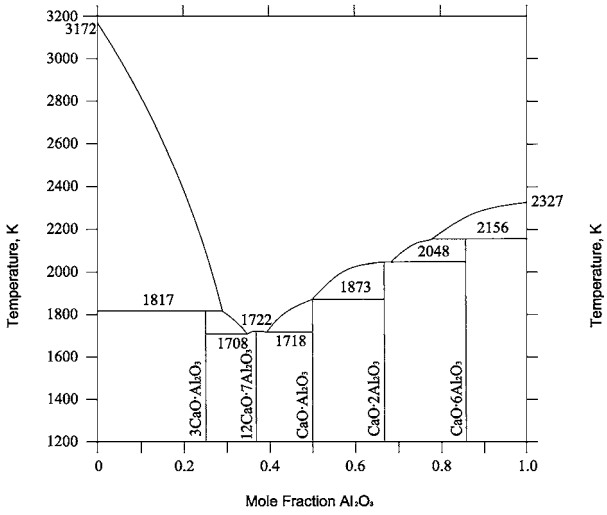


*Figure 1* Phase diagram of the $CaO–Al_2O_3$ system.

time. On the other hand, chemical synthesis using the sol-gel technology has also been used to produce these materials [7, 8, 14, 15]. Instead of using solid oxides as reactants, solutions containing calcia and alumina are first made (gel) and then heated at relatively low temperatures (e.g., <1173 K). This technique was normally used to produce powders or thin film of these compounds which are almost always in the amorphous state at low temperatures when prepared by the technique. Crystallization was then achieved by subsequent heating at higher temperatures. Tas [8] used a similar technique to prepare the liquid mixture, which was then placed in a muffle furnace at 783 K at which temperature the mixture undergoes boiling, dehydration, then glows to incandescence leading to a slow combustion (takes about 15 minutes). The product was still amorphous and subsequent sintering at high temperatures was required in order to obtain crystalline compounds.

In this work, the Self-Propagating High Temperature Synthesis (SHS), or Combustion Synthesis [16–18] is used to produce composites having matrices of these compounds. A typical SHS process involves formation of a green pellet from reactant powders and ignition of the pellet using an external heat source to generate a self-propagating combustion reaction. The SHS process can be realized by two modes, i.e., propagation (or combustion) mode and simultaneous (or thermal explosion) combustion mode. In the propagation mode, the reactants are ignited by an external heat source. Once ignited, the highly exothermic reaction ignites the next adjacent reactant layer by itself thereby generating a self-sustaining wave propagating toward the unreacted portion of the sample. In the simultaneous combustion mode, the reactants are heated uniformly until the combustion reaction is initiated simultaneously throughout the whole pellet. A combustion synthesis reaction is characterized by four parameters: the ignition temperature, combustion temperature, combustion wave velocity and the characteristics of the combustion wave. The ignition temperature is the temperature at which the reaction rate becomes appreciable leading to self-propagating reactions. The combustion temperature is the maximum temperature achieved, which is lower than the adiabatic temperature. The combustion wave velocity is the overall combustion rate, and the combustion wave characteristics describe the nature of the combustion wave, i.e., whether the combustion wave is stable or unstable. All these parameters are affected significantly by the properties of green pellets (i.e., particle size, green density, reaction environment, etc.) which have a profound influence on the combustion. In the SHS technology, the reactants are also solid powders but are usually different than those used in the traditional technique such as sintering. Obviously, the technique used by Tas [8] was different from the SHS process described above, although the author used the terminology of "Self-propagating Combustion Synthesis."

## 2. The SHS reactions

The combustion synthesis reactions are shown by the equation:

$$\mathrm{Ti} + \mathrm{B_2O_3} + \mathrm{Al} + \alpha\mathrm{CaO} \rightarrow \mathrm{TiB_2} + \mathrm{Al_2O_3} + \alpha\mathrm{CaO} + \Delta H_f^{T_0} \quad (1)$$

The self-propagating combustion reaction is sustained by aluminium reducing $B_2O_3$ at the combustion front forming the aluminium oxide ($Al_2O_3$), and the free boron (B) atoms then react with titanium (Ti) forming titanium diboride ($TiB_2$). This is a thermite-type reaction which releases a large amount of heat ($\Delta H_f^{T_0}$), enough to fuse the $Al_2O_3$ and CaO together forming a matrix consisting of $TiB_2$, $Al_2O_3$ and CaO phases. Clearly, in order to form the calcium-aluminate compounds, the reactions represented by Equation 1 must continue as:

$$\mathrm{TiB_2} + \mathrm{Al_2O_3} + \alpha\mathrm{CaO} + \Delta H_f^{T_0} \rightarrow \mathrm{TiB_2} + \mathrm{Ca_\alpha Al_2O_3} + \alpha + \Delta H_f^{T_0} + \Delta H_f^{T_0}(\mathrm{c}) \quad (2)$$

where $\Delta H_f^{T_0}(\mathrm{c})$ is the heat released in the process of compound formation and the values at room temperature are shown in Table I for all compounds in the system. Calcium-aluminate compounds are formed by proper selection of the $\alpha$ values in Equation 2, thus forming composites with calcium-aluminate compounds as the matrix and $TiB_2$ as the second phase. Table II shows the respective $\alpha$ values to form different calcium-aluminate compounds as the matrix phases and the overall composition in the final product. For example, to produce a sample with a matrix composition

TABLE II Adiabatic temperature and composition of final product (wt%) produced by reaction (1)

| Matrix ($CaO$–$Al_2O_3$) | $\alpha$ | Tad (K) | Compositions of products (wt%) | | |
|---|---|---|---|---|---|
| | | | $Al_2O_3$ | CaO | $TiB_2$ |
| $C_3A$ | 3.0 | 2160 | 30.0 | 49.5 | 20.5 |
| $C_{12}A_7$ | 1.7 | 2327 | 38.1 | 35.9 | 26.0 |
| CA | 1.0 | 2437 | 44.8 | 24.6 | 30.6 |
| $CA_2$ | 0.5 | 2650 | 51.1 | 14.1 | 34.8 |
| $CA_6$ | 0.17 | 2819 | 56.4 | 5.2 | 38.4 |

corresponding to the $C_{12}A_7$ compound, 1.7 moles of CaO is added to every mole of Al to be used, and the final product is a composite composed of 26 wt% $TiB_2$ and 74 wt% $C_{12}A_7$.

The adiabatic temperature ($T_{ad}$) is the maximum possible temperature without heat loss. It can be determined by the following equation [17–19]:

$$\Delta H_f^{T_0} = \int_{T_0}^{T_{ad}} \sum_i C(p_i)\,dT \tag{3}$$

where $\Delta H_f^{T_0}$ is the heat of formation at the temperature $T_0$, $C(P_i)$ is the heat capacity for the $i$th product, and $T_{ad}$ is the adiabatic temperature. If the ignition occurs at room temperature, then the heat of formation can be determined from standard heat of formations of products and reactants by $\Delta H_f^{298} = \sum_i [\Delta H_f^{298}(P_i) - \Delta H_f^{298}(R_i)]$. Using the thermodynamic data from Barin *et al*. [20], the adiabatic temperatures for the combustion reactions represented by Equation 1 for various compositions are calculated using Equation 3 and the results are also listed in Table II. It is noticed that the adiabatic temperatures for all compositions listed in Table II are higher than their melting points shown in Table I.

## 3. Experimental methods

Fine reactant powders were used in the present work and their specifications are shown in Table III. These powders were first weighed according to compositions determined by Equation 1 and then thoroughly mixed by ball milling for at least 4 hours. Cylindrical green pellets were then prepared by uniaxial pressing to a relative density of $58.6 \pm 0.7\%$ of its theoretical density. Each pellet had a diameter of 12.7 mm (0.5 inches) and weighed 2.5 grams.

The details of the experimental set-up were described in a previous work [21]. Briefly, the set-up included a combustion chamber and a fully automated ignition and data acquisition system. After a green pellet was loaded into the combustion chamber by placing it directly on top of the ignition coil, ignition was achieved using a computer-controlled power input into the tungsten coil in an ultra-high purity argon atmosphere. The control of the ignition power was considered to be crucial in obtaining reliable combustion parameters and pre-heating to the green pellet before ignition was controlled in a precise and repeatable manner. The data acquisition system recorded ignition power, temperature history, and pressure change during the whole combustion synthesis process. Two C-type thermocouples (W-5%Re/W-26%Re) of 0.005 inches in diameter (welded under flowing argon atmosphere) were used for temperature measurements. Finally, a video recording system, consisting of a digital camera, was used to record the whole combustion process from which the combustion wave velocity was determined.

TABLE III Specifications of the reactant powders

| Reactants | Particle size ($\mu$m) | Impurity (%) | Vendors |
|---|---|---|---|
| Aluminum (Al) | <45 | <0.5 | AlfaAesaer |
| Boron Oxide ($B_2O_3$) | <45 | <0.02 | AlfaAesaer |
| Calcium Oxide (CaO) | <45 | <0.01 | Cerac |
| Titanium (Ti) | <45 | <0.02 | Cerac |

All of the combustion reactions were ignited from the bottom of the samples to take advantage of the convection effect of argon [22]. The combustion wave velocity was determined by linearly fitting the wave front position (obtained from frame-by-frame measurement of the recorded combustion wave) versus time plot.

## 4. Results and discussion

### 4.1. Combustion characteristics

A typical combustion synthesis process involves ignition of a green pellet, formation of a self-propagating combustion wave, and cooling down. In the current work, ignition was achieved by resistance heating of a W-coil with high electrical current. Since both the combustion parameters (combustion temperature, wave velocity, and nature of the combustion waves) and microstructure of the product depend strongly on the characteristics of the ignition power [21], it is important to specify the ignition power profile being used. A typical ignition power profile for the present work is shown in Fig. 2 for a sample with a relative green density of 60% of theoretical and a matrix composition of $C_{12}A_7$. The ignition coil had a spiral configuration with a typical cold resistance of 58 m$\Omega$. At the time $t_i$, a pre-set power (voltage and current) was applied to the coil. As it was heated up, the resistance of the coil increased, resulting in more power input to the ignition coil. The power input to the ignition coil was terminated at the

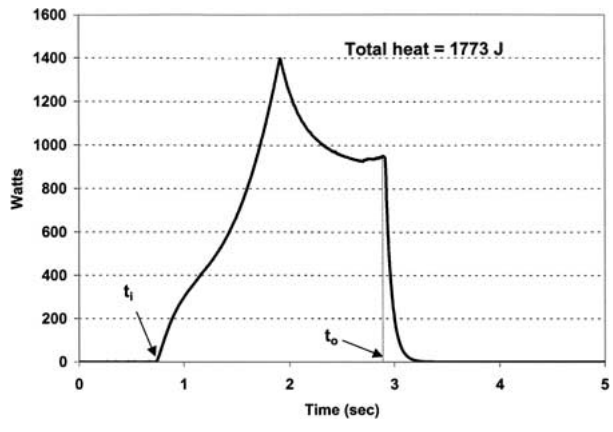


*Figure 2* A typical ignition power profile for a sample with a matrix composition of $C_{12}A_7$.

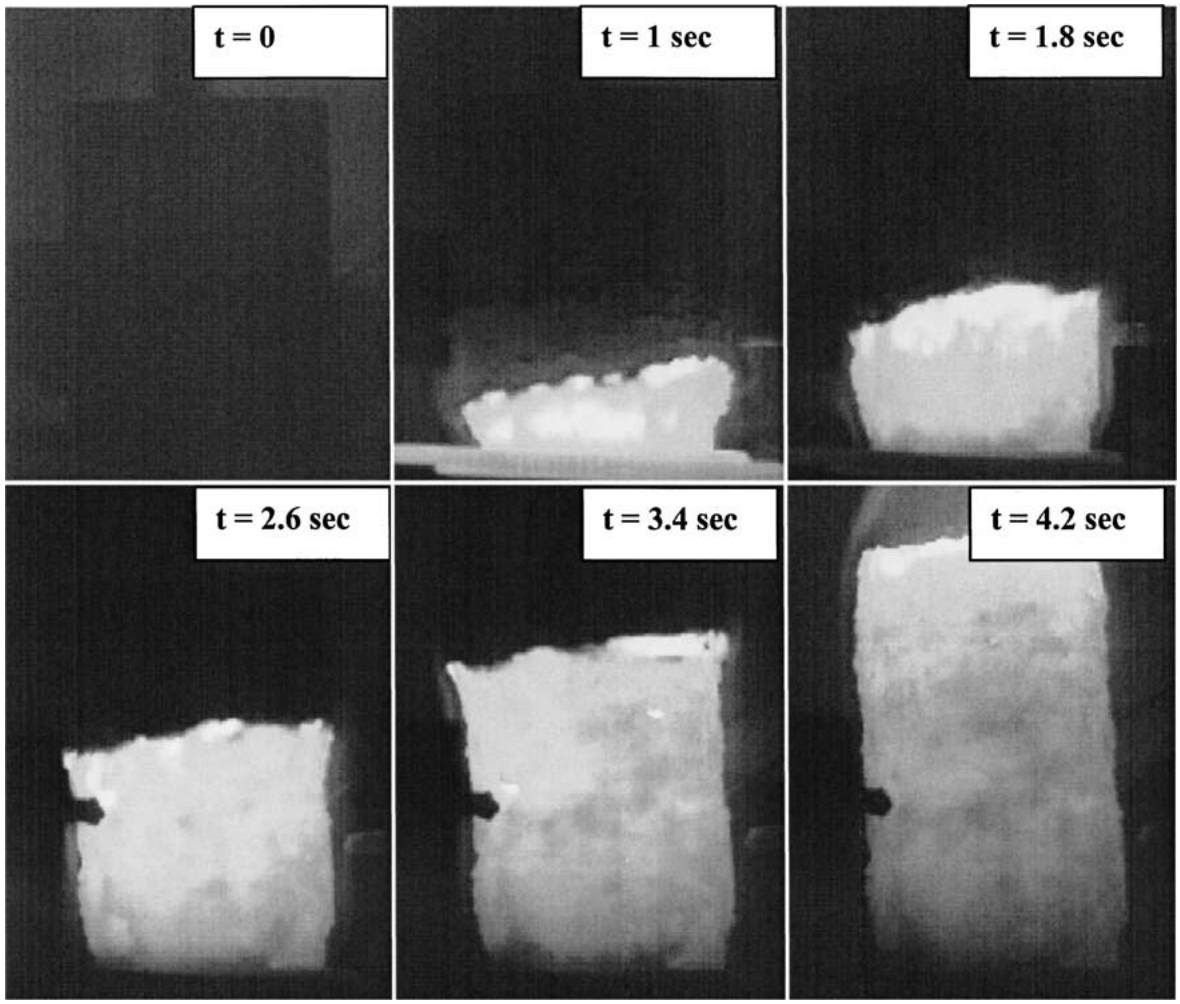


*Figure 3* Images of a typical combustion synthesis process for a sample with a matrix composition of $C_{12}A_7$.

pre-determined ignition time $t_0$. The ignition power was controlled precisely to allow a repeatable power profile for ignition, thus allowing both repeatable and predictable pre-heating to the green pellets.

Since the ignition power profile was exactly the same for all samples, only ignition energy had to be controlled in order to have repeatable effects on the green pellet. The ignition energy is the area under the curve in Fig. 2, which was 1773 Joules for this particular sample. The ignition energy for all of the samples in the present work was controlled to be $1793 \pm 52$ Joules. Using the ignition profile and energy, initiation of combustion waves was fairly easy for all compositions and a self-propagating combustion wave could be established for all compositions except the one with a matrix composition corresponding to $C_3A$. For this composition, although ignition could readily be achieved, the combustion wave stopped (quenched out) in all samples and self-propagating combustion reactions could only be achieved by higher ignition energy causing substantial preheating to the green pellet. Typical images of a combustion synthesis process are shown in Fig. 3 for a sample with a matrix composition of $C_{12}A_7$. After the ignition, the combustion synthesis reaction wave was initiated in a small layer of the pellet closest to the ignition coil. Since the combustion synthesis was an exothermic chemical reaction process, the heat released during reaction of the small layer would ignite the adjacent layer thus generating a self-propagating combustion wave propagating toward the unreacted part of the pellet. The combustion wave propagated along the longitudinal direction of the cylindrical pellet. A typical temperature profile is shown in Fig. 4. It can be seen that before the combustion synthesis reaction, the pellet was pre-heated to the temperature $T_p$. The combustion zone is a very narrow region, typically being 0.3 seconds (the time from $T_p$ to the combustion temperature $T_c$) and the product was formed in this narrow zone. Afterward, the reacted product cooled down.

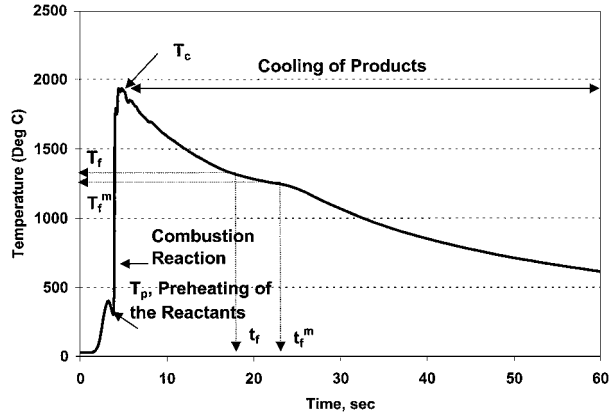


*Figure 4* Temperature change during the combustion synthesis process for a sample with a matrix composition of $C_{12}A_7$.

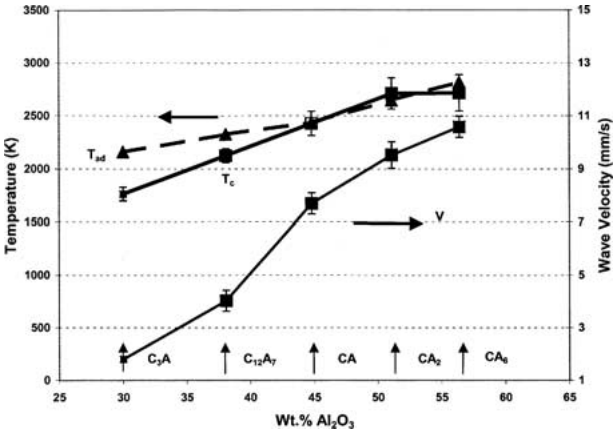


*Figure 5* The effects of composition on the adiabatic temperature ($T_{ad}$), combustion temperature ($T_c$), and combustion wave velocity ($V$).

Combustion temperature ($T_c$) and wave velocity ($V$) for all other compositions are shown in Fig. 5. For all compositions except $C_3A$, the combustion waves propagated in a stable manner with relatively high speed, from 4.0–10.6 mm/s. Both the $T_c$ and $V$ increase with the increase of the amount of $Al_2O_3$ due to increased exothermicity. It can also be seen that the combustion temperatures for the samples with matrix compositions of CA and $CA_2$ were very close to their adiabatic temperatures as shown in Fig. 5 (dashed line). This could be attributed either to the negligible heat loss, or the fact that the formation of compounds from individual oxides (Equation 3) releases extra heat which was not included in the adiabatic temperature calculations, or both. This is particularly true for the samples with a matrix composition of $CA_2$ since the average combustion temperature was 63 K higher than the adiabatic temperature. Except for the composition of $C_3A$, all other compositions had combustion temperatures higher than the melting points ($T_m$) of their respective compounds, as shown in Table IV. Therefore, a molten product had formed in the combustion front for these reactions.

From Fig. 4, it can be seen that there is a change in cooling rate of the reacted molten product at the time $t_f$ where the temperature curve starts to deviate from the baseline. The deviation is believed to be caused by solidification and crystallization of the $C_{12}A_7$ compound since the crystallization releases heat causing a slow down in cooling rate. This is more obvious from the plot of cooling rate ($dT/dt$) versus time as shown in Fig. 6 for the same curve shown in Fig. 4. The maximum crystallization rate occurs at the time $t_f^m$ and at the corresponding temperature $T_f^m$ . If the temperature at the time $t_f$ is defined as the freezing temperature ($T_f$), then the value of $\Delta T = T_m - T_f$ represents undercooling. The $\Delta T$ values for all compositions in the current work are shown in Table IV. As can be seen, the undercooling is relatively larger for the $C_{12}A_7$ compound. The implication of this on the tendency of glass formation will be discussed in another work.

TABLE IV Liquid formation ($T_c - T_m > 0$) and undercooling ($T_m - T_f$) of calcium-aluminate compounds during the combustion synthesis process

| Matrix compounds | $C_3A$ | $C_{12}Al_7$ | CA | $CA_2$ | $CA_6$ |
|---|---|---|---|---|---|
| $T_c - T_m$ | $-53 \pm 64$ | $407 \pm 66$ | $380 \pm 115$ | $665 \pm 198$ | $562 \pm 171$ |
| $\Delta T$ | — | $133 \pm 14$ | $24 \pm 37$ | $82 \pm 70$ | $73 \pm 129$ |
| $T_m - T_f^m$ | — | $191 \pm 33$ | $45 \pm 24$ | $134 \pm 65$ | $232 \pm 117$ |

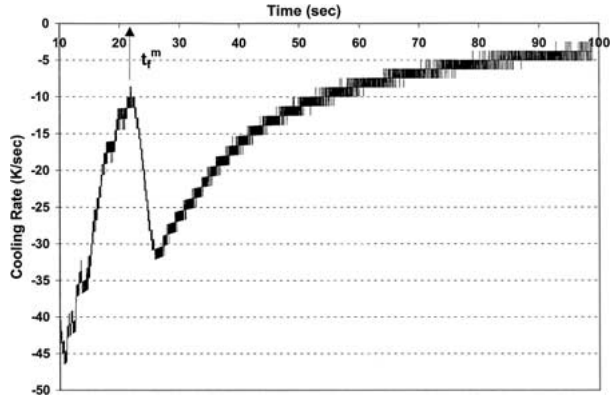


*Figure 6* Cooling rate of reacted product for the same sample shown in Fig. 4.

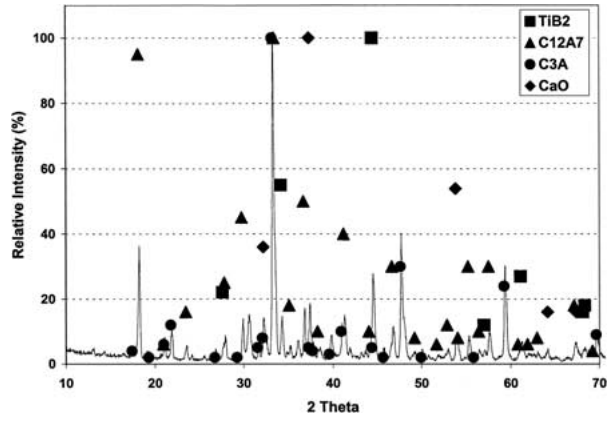


*Figure 7* The XRD spectra for a sample with a matrix composition of $C_3A$.

## 4.2. Microstructures

The X-ray diffraction (XRD) spectra for the sample corresponding to the matrix composition of $C_3A$ is shown in Fig. 7. Since a self-propagating combustion wave could not be established for this composition and the wave was quenched out during burning, the spectra were from a sample that went through repeated ignition (substantial pre-heating to the pellet occurred before achieving the final complete combustion). The equilibrium phase ($C_3A$) has clearly been formed, but the $C_{12}A_7$ phase has also formed in substantial amount. The CaO phase seems to be present as well. Therefore, it can be concluded that for this particular composition, Equation 1 has proceeded to completion (since no elemental aluminium exists in the spectra) but the subsequent reaction to form the $C_3A$ compound (Equation 3) only occurred partially. The XRD spectra for the sample with a matrix composition corresponding to $C_{12}A_7$ is shown in Fig. 8. The predominant phase in the matrix of the sample is the equilibrium $C_{12}A_7$ phase and a small amount of CA also exists. It seems that there also exists a small amount of another phase since there are extra peaks that cannot be assigned to either the $C_{12}A_7$ or the CA phase. This phase should be CaO-rich when

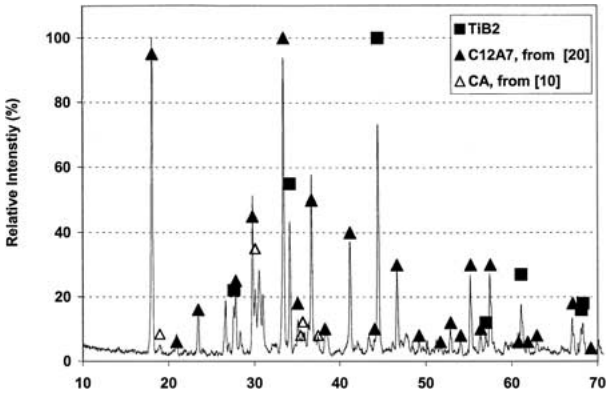


*Figure 8* The XRD spectra for a sample with a matrix composition of $C_{12}A_7$.

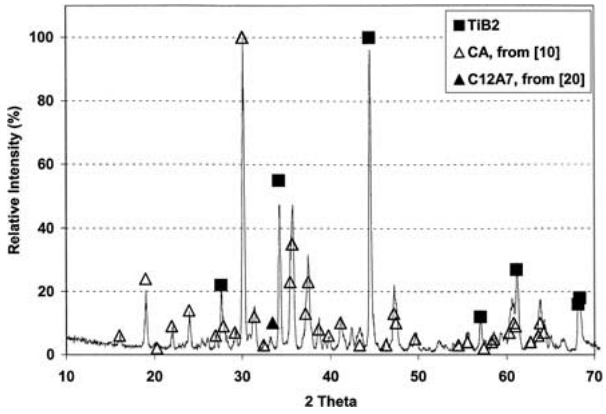


*Figure 9* The XRD spectra for a sample with a matrix composition of CA.

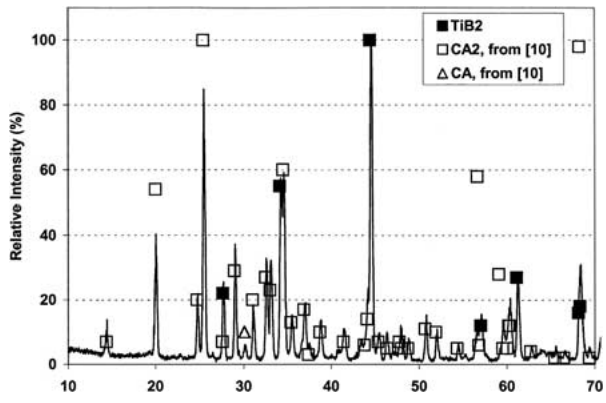


*Figure 10* The XRD spectra for a sample with a matrix composition of $CA_2$.

mass balance is considered. The XRD spectra for the sample with a matrix composition of CA is shown in Fig. 9. Clearly, almost pure CA compound has formed in the matrix. The same conclusion can be reached for the sample with a matrix composition of $CA_2$, as shown in Fig. 10. In Fig. 11, the XRD spectra for the sample with a matrix composition of $CA_6$ is shown. The phases formed in the matrix are $CA_2$ and $\alpha$-$Al_2O_3$ and there is no evidence of formation of the $CA_6$ compound.

From the microstructures indicated by these XRD spectra, it can be concluded that reaction (1) proceeded to completion for all compositions. However, the reactions represented by Equation 2 to form equilibrium pure compound phase occurring at their respective com-

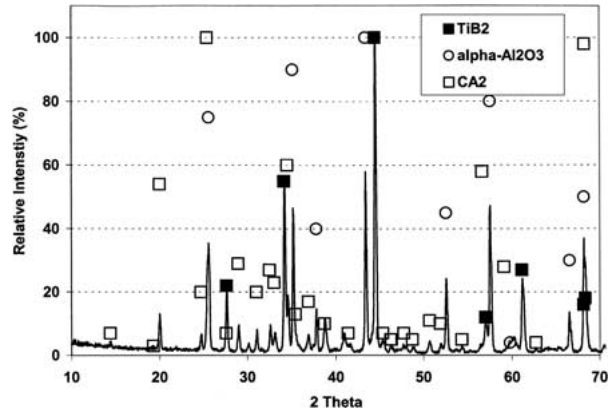


*Figure 11* The XRD spectra for a sample with a matrix composition of $CA_6$.

bustion temperature ($T_c$) inside a very narrow combustion front should be modified to:

$$
\begin{aligned}
3C + A &\xrightarrow{1764\ K} C_3A + C_{12}A_7 + C(m)\\
12C + 7A &\xrightarrow{2125\ K} C_{12}A_7 + CA(m)\\
C + A &\xrightarrow{2428\ K} CA + C_{12}A_7(m)\\
C + 2A &\xrightarrow{2713\ K} CA_2 + CA(m)\\
C + 6A &\xrightarrow{2718\ K} CA_2 + A
\end{aligned}
\qquad (4)
$$

Here, the m in brackets represents minor phase. Except for the $3C + A$ reaction, all other reactions shown in Equation 4 occurred in the liquid state. The liquid phase is ionic in nature consisting of cations ($Ca^{+2}$, $Al^{+3}$) and anions ($O^{-2}$) [23]. Obviously, the reactions represented by Equation 4 involve exchange of electrons between ions.

In general, a chemical reaction is dictated by thermodynamics and kinetics. According to the thermodynamic data [3, 9], all of the binary compound formation reactions represented by Equation 3 are thermodynamically favourable. However, the reaction rate is controlled by the kinetics, i.e., the activation energy or the diffusivity of the species involved. Clearly, both the $C_3A$ and $CA_6$ compounds show kinetics of slow reaction rate with $CA_6$ being the slowest since there was no evidence of this phase formation in the present work, even at a very high combustion temperature ($T_c = 2718$ K). The low reaction kinetics was also observed for the $C_3A$ compound when it was prepared via the solid reaction by sintering CaO and $Al_2O_3$ mixtures [6] and during crystallization of gel powders [7]. As for the $CA_6$ compound, although previous work showed that it was difficult to form below 1573 K [3, 24], it is still surprising that it is not formed at all at 2718 K in the present work.

## 5. Conclusions

1. The combustion synthesis reactions for synthesizing composites with matrices corresponding to binary calcium-aluminate compounds were highly exothermic with high combustion temperatures. As a result, the reacted products were in liquid states for all compositions

except the one corresponding to the matrix composition of $C_3A$.

2. The cooling of liquid product is characterized by relatively large undercooling under the current experimental conditions.

3. Almost pure compound matrix was formed for samples with a matrix composition of $C_{12}A_7$, CA, and $CA_2$. On the other hand, incomplete formation of $C_3A$ and no formation of $CA_6$ was observed. Therefore, the formation kinetics of $C_3A$ and $CA_6$ were slow with formation of $CA_6$ the slowest.

## Acknowledgements

This work was supported by the NASA Space Product Development Program through the Center for Commercial Applications of Combustion in Space at the Colorado School of Mines under NASA Cooperative Agreement Number NCCW-0096, and by the NASA Microgravity Research Division under Cooperative Agreement Number NCC3-659. Additional funding was provided by the Colorado Commission on Higher Education, the Colorado School of Mines and CCACS Industrial Partners CoorsTek, Guigne International Ltd, Hewlett-Packard, ITN Energy Systems and Sulzer Orthopedics Biologics. Experiments were assisted by Jonathan Curlett and Andrea Parrell.

## References

1. J. E. SHELBY, C. M. SHAW and M. S. SPESS, *J. Appl. Phys.* **66**(3) (1989) 1149.
2. G. A. RANKIN and F. E. WRIGHT, *Am. J. Sci.* **39** (1915) 1.
3. B. HALLSTEDT, *J. Amer. Ceram. Soc.* **73**(1) (1990) 15.
4. R. W. NURSE, J. H. WELCH and A. J. MAJUMDAR, *Trans. Br. Ceram. Soc.* **64** (1965) 323.
5. *Idem.*, *ibid.* **64** (1965) 409.
6. V. K. SINGH, M. M. ALI and U. K. MANDAL, *J. Amer. Ceram. Soc.* **73**(4) (1990) 872.
7. A. A. GOKTAS and M. C. WEINBERG, *ibid.* **74**(5) (1991) 1066.
8. A. C. TAS, *ibid.* **81**(11) (1998) 2853.
9. G. ERIKSSON and A. D. PELTON, *Metall. Trans.* B **24B** (1993) 807.
10. W. WONG-NG, H. McMURDIE, B. PARETZKIN, C. HUBBARD and A. DRAGOO, Powder Diffraction File, 38-1429.
11. Natl. Bur. Stan., *Circ.* **539**(9) (1960) 20, Powder Diffraction File, 09-0413.
12. P. J. BALDOCK, A. PARKER and I. SLADDIN, *J. Appl. Cryst.* **3** (1970) 188.
13. L. KELLER, J. RASK and P. BUSECK, Powder Diffraction File 38-0470.
14. M. UBEROI and S. H. RISBUD, *J. Amer. Ceram. Soc.* **73**(6) (1990) 1768.
15. M. A. GULGUN, O. O. POPOOLA and W. M. KRIVEN, *ibid.* **77**(2) (1994) 531.
16. A. MUNIR and U. ANSELMI-TAMBURINI, *Mater. Sci. Rep.* **3** (1989) 277.
17. J. J. MOORE and H. J. FENG, *Prog. Mater. Sci.* **39** (1995) 243.
18. H. C. YI and J. J. MOORE, *J. Mater. Sci.* **25** (1990) 1159.
19. H. C. YI, H. J. FENG, J. J. MOORE, A. PETRIC and J. Y. GUIGNÉ, *International Journal of SHS* **5**(1) (1996) 39.
20. I. BARIN, O. KNACKE and O. KUBASCHEWSKI, "Thermochemical Properties of Inorganic Substances" (Springer Verlag, 1977).
21. H. C. YI, J. Y. GUIGNÉ, J. J. MOORE, A. R. MANERBINO, L. A. ROBINSON and F. D. SCHOWENGERDT, "Combustion Synthesis of Glass ($B_2O_3$-$Al_2O_3$-MgO)-Ceramic($TiB_2$) Composites," *J. Mat. Synthesis Processing*, in press.
22. H. C. YI, T. C. WOODGER, J. J. MOORE and J. Y. GUIGNÉ, *Metall. Mater. Trans.* **29B** (1998) 889.
23. M. HILLERT, B. JANSSON, B. SUNDMAN and J. AGREN, *ibid.* **16A** (1985) 261.
24. H. VERWEIJ and C. M. P. S. SARIS, *J. Amer. Ceram. Soc.* **69**(2) (1986) 94.

*Received 30 January*
*and accepted 20 June 2002*